Self-organizing systems at finite driving rates

J. M. Carlson
Department of Physics, University of California, Santa Barbara, California 93106

E. R. Grannan
Department of Physics, University of California, Irvine, California 92717

G. H. Swindle
Department of Statistics and Applied Probability, University of California, Santa Barbara, California 93106
(Received 26 June 1992)

We consider finite driving-rate perturbations of models which were previously seen to exhibit self-organized criticality (SOC). These perturbations lead to more realistic models which we expect will have applications to a broader class of systems. At infinitesimal driving rates the separation of time scales between the driving mechanism (addition of grains) and the relaxation mechanism (avalanches) is infinite, while at finite driving rates what were once individual relaxation events may now overlap. For the unperturbed models, the hydrodynamic limits are singular diffusion equations, through which much of the scaling behavior can be explained. For these perturbations we find that the hydrodynamic limits are nonlinear diffusion equations, with diffusion coefficients which converge to singular diffusion coefficients as the driving rate approaches zero. The separation of time scales determines a range of densities, and, therefore, of system sizes over which scaling reminiscent of SOC is observed. At high densities the nature of the nonlinear diffusion coefficient is sensitive to the form of the perturbation, and in a sandpile model it is seen to have novel structure.

PACS number(s): 64.60.Ht, 02.50.+s, 05.40.+j, 05.60.+w

I. INTRODUCTION

A wide variety of spatially extended dissipative dynamical systems exhibit self-similar characteristics over a broad range of spatial and temporal scales. Observed scaling behaviors include the traditional power laws observed in, for example, the magnitude versus frequency distribution of earthquakes, as well as more exotic scalings such as multifractals which are observed in the growth patterns of diffusion-limited aggregates. The range of scales over which this behavior is observed in such systems is bounded *a priori* by both microscopic dimensions and times at one end and finite-size cutoffs at the other.

In traditional equilibrium statistical mechanics, scaling that extends up to the system size is characteristic of second-order critical points, and scaling that extends over a broad range is reminiscent of behavior near criticality. In the context of the open driven systems mentioned above, Bak, Tang, and Wiesenfeld [1] introduced the concept of "self-organized criticality" (SOC), in which the attractor of the dynamics intrinsically displays behavior on all scales without the obvious tuning of a parameter. The prototypical examples of such systems are referred to as sandpile cellular automata. In these models, "sand" is added one grain at a time to a randomly chosen site on a lattice. If the local scope (or height) exceeds a threshold, an avalanche is triggered, and sand falls according to a prescribed set of rules. Another grain is added to the pile only when the avalanche is complete, so that all sites are below threshold. The interesting characteristics shared by many of these systems are the lack of intrinsic temporal or spatial scales for the dynamics and a nontrivial scaling of the avalanche size distribution with system size [2–5].

While the sandpile models are easy to simulate, analytical progress remained elusive for quite some time, with the exception of Abelian models studied in, for example, Ref. [5]. However, recently Carlson *et al.* [6] introduced and studied a class of long-range particle-systems—two-state models—which exhibit nontrivial scaling like that observed in sandpile models. The two-state models have attributes that make them tractable mathematically. In particular, it was proven that the hydrodynamic limits of these self-organizing models are described by diffusion equations in which the diffusion coefficients have singularities at a critical density. This result led to a direct connection between the scaling in finite systems and an underlying critical phenomena in the thermodynamic limit [7]. It was shown that a key exponent—the order of the diffusion pole—identified various scaling properties of the open driven systems [8]. More generally, the presence of a singularity in the diffusion coefficient led to an explanation of why these systems approach the critical point as the system size diverges. Many of the results that were obtained analytically for the two-state models were seen numerically to apply to a variety of sandpile models as well [8,9]. For a particular sandpile model, referred to as the limited local sandpile model [2], there has been some additional recent analytical progress in obtaining various scaling properties that are associated with the diffusion limit [10,11]. Thus we have recast the criterion

for self-organized criticality, namely, the nontrivial scaling of spatial features, temporal signals, and event size distributions with the system size, in terms of singular diffusions, where SOC is associated with the existence of a diffusion singularity in the hydrodynamic limit and the approach to the critical density as the system size diverges.

In the two-state models, the diffusion singularities arose because a conserved quantity could be transported arbitrarily long distances instantaneously. The analogous behavior in sandpiles is associated with the feature that new grains of sand are added only after each avalanche is complete. This is commonly referred to as the limit of infinitesimally small driving rates for these models. As we shall see, this appears to be a necessary ingredient for self-organized *criticality* in the strictest sense; in particular, this feature is required to obtain a singularity in the diffusion coefficient. However, as we shall also see, this does not mean that the systems are devoid of interesting scaling if the driving rate is small but positive. One should not reach the conclusion that by tuning the driving rate to zero one has tuned the system to a critical point. In fact, at zero driving rate, both closed systems and open systems with injudiciously chosen boundary conditions will *not* approach the singularity as the system size diverges, and no interesting scaling will be seen. Self-organized criticality arises, at least in many cases, as a consequence of a singular diffusion coefficient in conjunction with appropriate boundary conditions (or, equivalently, driving mechanisms). The main point of this paper is to examine what happens to the scaling of the zero-driving-rate systems with nontrivial boundary conditions when the driving rate becomes positive.

Here we consider extensions of the two-state models and sandpiles to finite driving rates. In each case mass transport is no longer instantaneous, and what previously would have been individual avalanches may overlap. In these extensions we consider models that, like the sandpile models, can be described in terms of local rules. We expect that these extensions will be useful as we apply these techniques to other more realistic models where typically the separation of times scales is not infinite. At finite driving rates the diffusion coefficient will no longer be singular, although it can retain much of its structure. We will show how a separation of time scales determines the range over which nontrivial scaling is observed, with a crossover to some other behavior at larger system sizes. Because the extension to finite driving rates is not unique, we explore various extensions, and find that quite different behaviors are associated with different models.

The organization of the paper is as follows. In Sec. II we describe generalizations of the two-state models to finite driving rates and determine the associated diffusion coefficients. We will focus on cases for which analysis is possible (details are relegated to the Appendix). In Sec. III we describe numerical analysis of these models based on tracking the motion of tagged particles. Previously we proved that in the case of infinitesimal driving rates, the long-time behavior of tagged particles provides a convenient means of locating singularities in transport coefficients. Here we examine both the long-time and short-time behavior of tagged particles in the finite-driving-rates models. The short-time behavior is the analog of avalanches, and we observe a scaling crossover as system size is increased. In Sec. IV we consider the generalization of a particular sandpile model to finite driving rates where a diffusion coefficient with surprisingly rich structure is found. We conclude with a summary of our results in Sec. V.

II. GENERALIZATIONS OF THE TWO-STATE MODELS

A. Two-state models

We begin with a description of the class of self-organizing two-state models which were introduced and studied in Ref. [6]. On a lattice of N sites ($i=1,\ldots,N$) at time t, sites are either occupied [$h_t(i)=1$] or vacant [$h_t(i)=0$]. The system evolves according to the following rules. At rate $c(k)$ each 1 hops instantaneously to the nearest vacant site to the left, where k is the distance between the 1 and the vacant site. The same rule applies for instantaneous jumps to the right. In Ref. [8] the case $c(k)=1$, where the jump rate was independent of distance, was specifically considered, whereas in Ref. [6] the more general case, where $c(k)$ was a nonincreasing function of k, was considered.

The two-state models on a closed system with periodic boundary conditions were analyzed rigorously. It was proven that the usual diffusion scaling [12] led to a hydrodynamic limit in which the particle density $\rho(t,x)$ satisfies a diffusion equation of the form

$$\frac{\partial\rho}{\partial t}=\frac{\partial}{\partial x}\left[D(\rho)\frac{\partial\rho}{\partial x}\right], \tag{1}$$

where as $\rho\rightarrow 1$ the diffusion coefficient $D(\rho)$ has a singularity

$$D(\rho)\sim\frac{1}{(1-\rho)^{\phi}}. \tag{2}$$

In Eq. (2) the order of the pole is related to the rate of decay of the jump rates: when $c(k)\sim k^{-\alpha}$ for large k, we have $\phi=3-\alpha$ for $\alpha\geq 0$.

In these models jumps play the role of avalanches in the sandpile models. When we say that jumps take place instantaneously, it is the analog of viewing avalanches in sandpiles as long-range interactions that take place instantaneously relative to the rate at which sand is added to the system. Here we will consider generalizations of two of these models to the case where the jumps are no longer instantaneous. We will focus our attention primarily on the two-state model with $c(k)=1/k$, which we will refer to as the $1/k$ model. We will also mention perturbations of the $c(k)=1$ model. It is important to note that the reasons that we select these two is that in these systems any transition can be thought of as iterating a local rule, just as in sandpile models. In that sense, these models may be viewed as the most realistic of the two-state models. In addition, this feature will be useful when we modify the model so that long-range transitions, which used to take place instantaneously, now require

finite time. For example, in the $1/k$ model one can think of each 1 as hopping at rate one to a nearest-neighbor site on the left or right with equal probability. If this site is occupied then at rate $\lambda=\infty$ the 1 executives a symmetric random walk (SRW) until it hits a vacant site. It is easy to show that the probability that a SRW starting at site $n=1$ hits site $k>1$ before it hits the origin is $1/k$, which is how the rates $c(k)=1/k$ arise [13]. The limit $\lambda=\infty$ is a formal device for indicating that these transitions over occupied sites occur instantaneously. Similarly, the $c(k)=1$ model can be described in terms of local rules. In this case, rather than executing a symmetric random walk, the 1 performs a completely asymmetric random walk in the direction of its initial hop.

Remark. To arrive at similar descriptions for models with other transition rates [$c(k)=1/k^{\alpha}$ where $\alpha\neq 0,1$] in terms of local rules, one might suggest that iteration of an asymmetric random walk (with probability $p>\frac{1}{2}$ of jumping away from the initial site) would give the desired result. However, the resulting $c(k)$ is given by $c(k)=(1-\gamma)/(1-\gamma^k)$, where $\gamma=(1-p)/p$. Consequently, for large jump sizes k the rate $c(k)$ approaches a constant, and as a result the diffusion coefficient differs insignificantly from that for $c(k)\equiv 1$. In both cases the pole in $D(\rho)$ is third order.

B. Extension to positive driving rate

We must now construct models with $\lambda<\infty$. This amounts to making the long-range transitions (or avalanches), which in the two-state models are instantaneous, take a positive time to occur. We do this by viewing the long-range jumps as a sequence of nearest-neighbor jumps which become instantaneous in the limit $\lambda\to\infty$. Unless explicitly stated otherwise, we will be referring to the $1/k$ model. The appropriate generalization is clear once we decide what happens when the height at a site i exceeds 2: $h_t(i)>2$. We will examine two natural generalizations:

λ *model.* In this model, if $h_t(i)\geq 2$, then at rate λ the number of particles at the site i drops by one and the number of particles at $i-1$ or $i+1$, selected randomly, increases by one (i.e., a single particle hops). Specifically, the rates are

$$\begin{aligned} &h_t(i)\to h_t(i)-1 \\ &h_t(i+e)\to h_t(i+e)+1 \end{aligned} \quad \text{at rate} \quad \begin{cases} 0 & \text{if } h_t(i)=0 \\ 1 & \text{if } h_t(i)=1 \\ \lambda & \text{if } h_t(i)\geq 2\,, \end{cases} \tag{3}$$

where e denotes a symmetric random variable (i.e., $e=\pm 1$ with equal probability for each of the nearest-neighbor jumps). The key feature of this model is that the transition rate is fixed at λ for any site which is above threshold, and is thus independent of how far above threshold the site may be.

$n\lambda$ *model.* In this model, the number of particles at a site drops by one at rate $(n-1)\lambda$ if $h_t(i)=n\geq 2$, so that the transition rates are

$$\begin{aligned} &h_t(i)\to h_t(i)-1 \\ &h_t(i+e)\to h_t(i+e)+1 \end{aligned} \quad \text{at rate} \quad \begin{cases} 0 & \text{if } h_t(i)=0 \\ 1 & \text{if } h_t(i)=1 \\ (n-1)\lambda & \text{if } h_t(i)=n\geq 2\,, \end{cases} \tag{4}$$

with e defined above. The key feature of this model is that the transition rate continues to increase with increasing occupation of the site.

Of course, other finite-driving-rate extensions are possible. For example, we have also considered an alternative to the $n\lambda$ model above, in which sites with $n\geq 2$ particles drop at rate $n\lambda$ rather than $(n-1)\lambda$. While both versions sound very similar, the corresponding diffusion coefficients differ in the neighborhood of the diffusion singularity of the unperturbed model [14]. We have also considered a jump rate of $1+(n-1)\lambda$, so that the first particle on a site continues to jump at rate 1, while all additional particles jump at rate λ. The hydrodynamics of this model is very similar to our selected perturbation above; however, the task of computing the diffusion coefficient is substantially more complicated [15].

Remark. One should notice that λ and $n\lambda$ versions are possible for the $c(k)=1$ model, if e is changed to take a fixed value $+1$ or -1 determined by the direction of the initial jump. Note that we have lost the Markov property, unless we append a spin to each particle indicating a direction of motion, and, even after doing this, the processes are not reversible—a fact which seriously impedes analysis. This is not the case for the $1/k$ model, since the direction of a supercritical 1 is randomly selected for each jump. Consequently, the perturbations of the $1/k$ model are simply specific forms of the zero-range process previously studied in, e.g., Refs. [16,17]. These models are mathematically tractable, and as a consequence we are focusing almost exclusively on them.

C. Diffusion limits

We will now discuss hydrodynamic limits of the λ and $n\lambda$ versions of the $1/k$ model. The difference in the transition rates for the two versions will result in substantially different behavior at densities exceeding unity.

A rigorous analysis of the $n\lambda$ version is given in the Appendix, where we discuss the following theorem, which we state after introducing a few essential facts.

The content of the theorem is that, properly rescaled, the particle density of the system is described by a diffusion limit. Furthermore, as $\lambda \to \infty$ the diffusion coefficient converges to the singular diffusion coefficient of the original two-state model for all densities $\rho < 1$.

We consider the systems on an N-site torus $\mathcal{T}_N = \{1/N, \ldots, N/N\}$. In the invariant measures (equilibria) of each version of the $1/k$ model the distributions of the number of particles at two different sites are independent and identical. Since particles are conserved, there is a family of invariant measures indexed by the particle density $\rho \geq 0$, where $\rho = E[h(i)]$ is the expected number of particles per site. At a density ρ we will denote the equilibrium distribution of the number of particles on each site by $d_\rho(k)$, so that $P(h_t(i)=k) = d_\rho(k)$. In the Appendix d_ρ is calculated explicitly in terms of the transition rates.

The initial, nonequilibrium distribution of the system is described by a density profile $\gamma(x)$, namely, each site is initially occupied independently according to d_γ: $P(h_t(i/N)=k) = d_{\gamma(i/N)}(k)$. We denote by $\mathcal{P}_N^\gamma$ the path measure of the process. The limiting diffusion equation describes the relaxation of the nonequilibrium distribution to the invariant measure with the same average density. Since the particle system is discrete for any N, we must make the convergence statement in the weak sense, namely, via the action on smooth test functions.

Theorem. For the $n\lambda$ model there exists a function $D_{n\lambda}(\rho)$ (the diffusion coefficient) so that for any $G \in C^2(\mathcal{T})$ (twice differentiable functions on the torus) and any $\delta > 0$:

$$\lim_{N\to\infty} \mathcal{P}_N^\gamma \left[\left| \frac{1}{N} \sum_{i=1}^{N} G\left(\frac{i}{N}\right) h_{N^2 t}\left(\frac{i}{N}\right) - \int_{\mathcal{T}} G(x)\rho(t,x)\,dx \right| > \delta \right] = 0 , \tag{5}$$

where $\rho(t,x)$ is the solution of

$$\frac{\partial \rho}{\partial t} = \frac{\partial}{\partial x}\left[D_{n\lambda}(\rho) \frac{\partial \rho}{\partial x} \right] \tag{6}$$

with initial condition $\rho(0,x) = \gamma(x)$.

Remark. The proof of this result follows directly from the methods developed in Ref. [18] for coupled, nonlinear diffusions. The λ model is omitted in the theorem due to the absence of exponential moment conditions needed in the proof. However, we anticipate the validity of the diffusion limit in this case also, and the associated diffusion coefficient $D_\lambda(\rho)$ can be identified. In the Appendix we summarize the calculations which lead to implicit formulas for $D_\lambda(\rho)$ and $D_{n\lambda}(\rho)$ in terms of the transition rates. The basic properties of these diffusion coefficients are described below.

In Fig. 1 we plot the diffusion coefficients $D_\lambda(\rho)$ and $D_{n\lambda}(\rho)$. Note that for relatively small values of ρ both diffusion coefficients mimic the behavior of the singular ($\lambda = \infty$) diffusion coefficient $D(\rho)$, which is also shown. The singular diffusion coefficient diverges at $\rho_c = 1$; however, in both the λ and $n\lambda$ models there is a crossover in behavior at $\rho = \rho^*(\lambda) > \rho_c$. In the $n\lambda$ model the crossover is to linear diffusive behavior, where $D_{n\lambda}(\rho)$ is nearly constant, while in the λ model there is a peak in $D_\lambda(\rho)$ at ρ^*, followed by a sharp decline. In each case the value of D at the crossover is proportional to λ, and as $\lambda \to \infty$ we observe that $\rho^* \to \rho_c$, as one would expect. These facts are summarized in the following results, which are described in more detail in the Appendix.

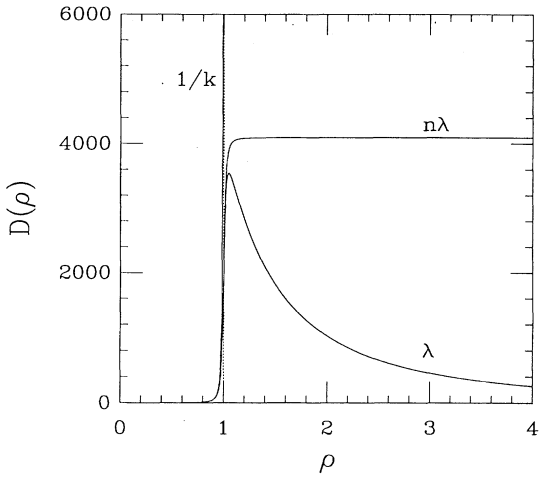

FIG. 1. Diffusion coefficients for the $1/k$ model and the associated λ and $n\lambda$ models as a function of density ρ for $\lambda = 8192$. For the $1/k$ model, $D(\rho)$ has a second-order pole at $\rho = 1$. At small densities, $D_\lambda(\rho)$ and $D_{n\lambda}(\rho)$ mimic the behavior of $D(\rho)$. Above $\rho = 1$, $D_\lambda(\rho)$ and $D_{n\lambda}(\rho)$ cross over to different behaviors, and as $\rho \to \infty$, $D_\lambda \to 0$ and $D_{n\lambda} \to \lambda/2$.

(a) $D_\lambda(\rho)$ and $D_{n\lambda}(\rho)$ converge to $D(\rho) = \frac{1}{2}(1-\rho)^{-2}$ as $\lambda \to \infty$ for all $\rho < 1$.

(b) $\lim_{\rho\to\infty} D_{n\lambda}(\rho) = \frac{1}{2}\lambda$; $\lim_{\rho\to\infty} D_\lambda(\rho) = 0$ [more precisely, $\lim_{\rho\to\infty} \rho^2 D_\lambda(\rho) = \frac{1}{2}\lambda$].

(c) For the λ model, letting ρ^* denote the location of the maximum of $D_\lambda(\rho)$ as a function of ρ, we have $\rho^* \sim 1 + \lambda^{-1/3}$.

The qualitative difference between the diffusion coefficients of the λ and $n\lambda$ models is easily understood. We emphasize this difference as it elucidates the fact that extensions of self-organizing models to finite driving rates can be made in many ways, and the behaviors of the various extensions are by no means guaranteed to be the same. In the $n\lambda$ model a crossover to simple linear diffusion is seen as follows. When a site is occupied by $n \geq 2$ particles, the jump rate per particle is $(n-1)\lambda/n$, so that as n becomes large this rate becomes independent of n; i.e., interactions decrease. In other words, in the high-density limit particles are essentially executing random walks at a transition rate λ, with the resulting limiting value of D being $\frac{1}{2}\lambda$.

In contrast, for the λ model, when a site is occupied by $n \geq 2$ particles the jump rate per particle is λ/n. So, as the density increases the mobility of individual particles actually decreases. To understand the impact of this on the diffusion coefficient, recall Fick's law, namely, that the diffusion coefficient D relates the linear response of the flux I to the density gradient ϵ: to leading order

$I \sim \epsilon D$. In the λ model, because the transition rate is independent of n for sites with $n \geq 2$ particles, the only net contributions to the flux arise from adjacent sites, at least one of which is occupied by fewer than two particles. As the density increases these sites become increasingly rare. Therefore the flux and the diffusion coefficient decrease to zero as $\rho \to \infty$.

Remark. As previously stated, for the corresponding diffusion descriptions of perturbations to the $c(k)=1$ two-state model, the lack of reversibility impedes rigorous analysis. Nevertheless, one would expect that the diffusion coefficient would have a similar appearance for small densities, with more rapidly increasing $D_\lambda(\rho)$ and $D_{n\lambda}(\rho)$ for $\rho < \rho^*$, in accord with the higher-order singularity when $\lambda = \infty$. However, we expect that the large-density asymptotics of the diffusion coefficient for the $n\lambda$ version of this system differs substantially from the diffusion coefficients associated with the corresponding perturbations of the $1/k$ model. For perturbations of the $c(k)=1$ model, once a particle starts hopping in a given direction, it continues in that direction until it hits an empty site. At high densities empty sites become increasingly rare so that rather than approaching a limiting constant the diffusion coefficient should increase without bound as $\rho \to \infty$.

D. Density profiles on the open driven systems

Next, as we did previously for the two-state models in Ref. [8], we apply the results obtained here for the closed system to the open system with appropriate boundary conditions. In particular, we solve

$$\frac{d\rho}{dt} = \frac{d}{dx}\left[D(\rho)\frac{d\rho}{dx} \right] \tag{7}$$

to obtain the steady-state profile ($d\rho/dt = 0$) subject to the boundary conditions $\rho(1)=0$ and $\rho'(0)D(\rho(0)) = -\alpha N \equiv -\alpha_N$. As before, the second condition arises from the input flux at rate α at the origin in the (unrescaled) discrete model. The factor of N comes from the diffusion scaling [8] [(flux)=(mass)(rate)$=N^{-1}N^2=N$]. First, we describe the solution to the boundary-value problem for the unperturbed systems with singular diffusion limits.

Behavior of the two-state models ($\lambda = \infty$)

In the two-state models with a diffusion singularity of the form $D(\rho) \sim \frac{1}{2}(1-\rho)^{-\phi}$ (the factor of $\frac{1}{2}$ is inserted for consistency with the finite-driving-rate versions, in which particles select a direction to move with probability $\frac{1}{2}$ each) we obtain a solution for $\phi > 1$ of the form

$$\rho(x) = 1 - [1 + 2\alpha N(\phi-1)(1-x)]^{-1/(\phi-1)} , \tag{8}$$

which is illustrated for the $1/k$ model ($\phi = 2$) in Fig. 2(a) for a variety of system sizes N. Note that the increase in the effective driving rate α_N with system size N leads to profiles which approach the singularity at $\rho = \rho_c = 1$ as $N \to \infty$. To satisfy the boundary condition at $x = 1$ there is a boundary layer with width of order $1/N$ at the open edge of the system.

Behavior of the λ and $n\lambda$ models. For the $\lambda < \infty$ models, the same boundary conditions again lead to an increasing average density with increasing system size (see Fig. 2). Notice that at low densities the profiles of both the λ and $n\lambda$ models are nearly indistinguishable from the $\lambda = \infty$ case, which is consistent with similar behavior in the diffusion coefficients observed in Fig. 1. However, as N increases we begin to see departures of the λ and $n\lambda$ models from the corresponding two-state model and from one another, which reflect the differences in the diffusion coefficients at high densities. In each case, the crossover behavior sets in when the system size is of order $\lambda^{1/2}$, at which point the fact that λ is finite will begin to affect the dynamics significantly and lead to overlapping events. To see that this is the appropriate scaling of the crossover, note that when $\lambda = \infty$, the average density scales as $\bar{\rho} \sim 1 - 1/N$, so that the average distance between 0's is of order N. A random walker takes of order N^2 jumps to move a distance N, implying that a typical "event" for the $\lambda < \infty$ model requires an average time of N^2/λ. Therefore one would expect to see many supercritical sites (overlapping events) when $N \sim \lambda^{1/2}$.

One can also estimate the crossover using the hydrodynamic limit. The constant flux condition, which is satisfied at each point x in the stationary solution, can be applied at the right edge $x = 1$. That, along with the open edge condition $\rho(1)=0$, implies the existence of a boundary layer of thickness $\sim 1/N$. Specifically, for any fixed number $\hat{\rho} < 1$, the location $x_{\hat{\rho}}$ at which $\rho(x_{\hat{\rho}}) = \hat{\rho}$ scales like $x_{\hat{\rho}} \sim 1 - b/N$ with b a constant. If we take $\hat{\rho}$ close to unity then for the $n\lambda$ model across the rest of the system ($0 \leq x < 1 - b/N$) the linear diffusion equation is a good approximation and the flux condition becomes

$$\tfrac{1}{2}\lambda\rho' \approx -\alpha N , \tag{9}$$

where we have substituted the asymptotic form of the diffusion coefficient $D(\rho) \approx \frac{1}{2}\lambda$. So, away from the boundary layer we have

$$\rho(x) \approx \frac{2\alpha N}{\lambda}[1-x] + \hat{\rho} - \frac{2\alpha b}{N} , \tag{10}$$

namely, a linear decay starting from the left edge. Comparing this to the stationary solution for the two-state model (8), we see that corrections to the density $\rho(x)$ from the $\lambda = \infty$ profile are of order N/λ. Crossover occurs when the profile exceeds unity. The fact that the unperturbed profile scales like $1 - 1/N$ implies once again that the crossover occurs when $\lambda \sim N^2$.

In the λ model with the boundary conditions specified above, similar arguments reveal that as N increases a region of extremely high density develops at the left side of the system. In fact, beyond some critical system size the density diverges with time and no stationary solution exists. The essential change is that, instead of (9), one has

$$\frac{\lambda}{2\rho^2}\rho' = \alpha N . \tag{11}$$

Integrating toward $x = 0$, one finds that the solution becomes singular when $\alpha N > \frac{1}{2}\lambda$. In fact, it is easy to prove the absence of a stationary solution when the system size exceeds $\lambda/2\alpha$:

Claim. Given the boundary conditions above, no stationary solution for the λ model exists when the system size exceeds $N_{\max}=\lambda/2\alpha$.

To prove this, let $r(k)$ denote the rate at which a particle leaves a site with k particles [$r(k)=1$ when $k=1$; $r(k)=\lambda$ when $k>1$], and if we let $P_i(k)$ denote the probability that site i has k particles in a stationary state, then the flux between neighboring sites must be α:

$$\tfrac{1}{2}\sum_{k=1}^{\infty} P_i(k)r(k)-\tfrac{1}{2}\sum_{k=1}^{\infty} P_{i+1}(k)r(k)=\alpha \tag{12}$$

for $1\le i\le N-1$, and

$$\tfrac{1}{2}\sum_{k=1}^{\infty} P_N(k)r(k)=\alpha \tag{13}$$

at the open edge. Solving backwards from site N we find

$$\tfrac{1}{2}\sum_{k=1}^{\infty} P_1(k)r(k)=N\alpha\ . \tag{14}$$

Finally, note that we have an upper bound of λ for the sum, which implies that for any $N>\lambda/2\alpha$ no stationary solution exists.

In simulations particles continue to pile up, leading to a diverging density. This is another manifestation of the decreasing mobility of individual particles with increasing density seen first in $D_\lambda(\rho)$ (Fig. 1). For this reason the λ model with these boundary conditions is ill-posed for large system sizes. Of course, this behavior can be avoided by specifying different boundary conditions, such as fixed densities at both sides, although this will be devoid of the crossovers that we are studying. One motivation for studying the λ model is that the associated diffusion coefficient is in some ways quite similar to that of the perturbation of the sandpile model that we consider below, which also exhibits similar difficulties at large system sizes.

Finally, on the open system the differences between the three models—the two-state model and the associated λ

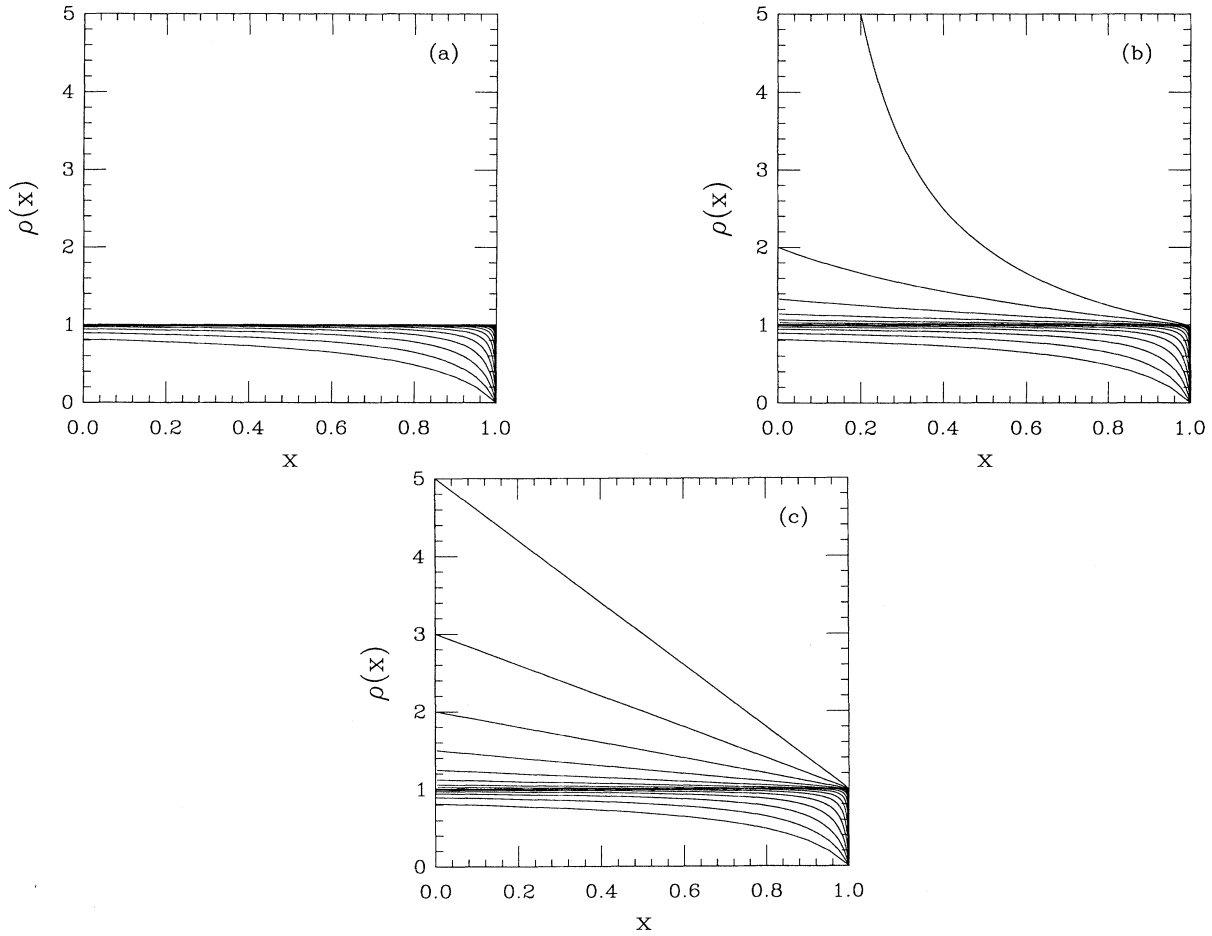

FIG. 2. Density profiles for the open systems. (a) Our analytical solutions for the $1/k$ model with appropriate boundary conditions, for $N=2,4,8,16,\ldots,16\,384$ and $\alpha=1$. The lowest curve corresponds to the smallest value of N, and the density increases monotonically with increasing N. (b) and (c) The corresponding results for the λ and $n\lambda$ models, respectively, with $\lambda=8192$. While one would not expect hydrodynamics to hold on the smallest of these system sizes, we can still construct analytical profiles. For small values of N we observe similar scaling in all three models; however, at system sizes $N\sim\lambda^{1/2}$ we begin to see crossover behavior which is associated with the fundamental differences in the associated diffusion coefficients (Fig. 1). No solution can be obtained for the λ model when $N>\lambda/2\alpha$.

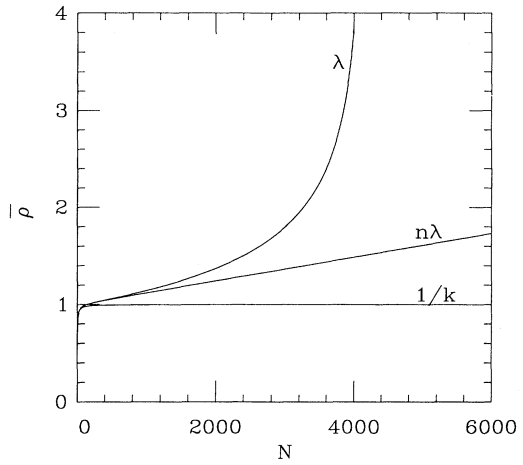

FIG. 3. Average density as a function of system size N for the $1/k$ model and the associated λ and $n\lambda$ models ($\lambda=8192$). The average density is derived from the analytical calculations which also lead to the profiles illustrated in Fig. 2. For small N all three models behave the same. However, for large N in the $1/k$ model the density approaches unity, in the $n\lambda$ model the density scales with N, and in the λ model the density diverges when $N=\lambda/2\alpha$.

and $n\lambda$ models—is summarized by considering the system-wide average density $\bar{\rho}$ as a function of N, as illustrated in Fig. 3. For relatively small system sizes all three models behave similarly, following the behavior of the two-state model, which was seen previously to scale as

$$\bar{\rho}\sim 1-1/N^{1/(\phi-1)} . \tag{15}$$

In the two-state model $\bar{\rho}$ approaches the critical point $\rho_c=1$ as $N\to\infty$. However, for the λ model we have shown that the density diverges with time when the system size is too large (of order λ). Finally, for the $n\lambda$ model we have shown that there is a crossover at $N\approx\chi^{1/2}$ beyond which

$$\bar{\rho}_{n\lambda}\sim\frac{\alpha N}{2\lambda} . \tag{16}$$

As we will see in the next section, these scaling crossovers are also manifested in other aspects of the dynamics.

III. TAGGED PARTICLES AND SCALING CROSSOVERS

One numerical method that can be used to identify singularities in transport coefficients in these and other diffusive systems involves introducing and subsequently monitoring the decay of small amplitude perturbations [8]. In particular, on a closed system with periodic boundary conditions for any density of the conserved quantity ρ, there is a translation-invariant equilibrium with density ρ to which the system relaxes from other initial distributions. When a small amplitude perturbation is introduced, it is easily verified from the linearized version of Eq. (7) that each Fourier mode of the perturbation relaxes to zero exponentially at a rate proportional to $D(\rho)$. Thus by varying the average density ρ of the initial condition the density dependence of the diffusion coefficient can be extracted.

In our previous analysis we have used this relaxation method extensively; however, it is not without its difficulties in implementation. These are primarily associated with the fact that it is intrinsically a nonequilibrium measurement. For example, care must be exercised to guarantee that perturbations are small enough to remain in the linear regime, which at densities near a singularity makes the decay of the perturbation more difficult to measure. In this section we use the behavior of tagged particles to explore various aspects of the dynamics of the systems studied in Sec. II. Monitoring the long-time behavior of tagged particles provides an alternate method of locating singularities in the transport coefficients. This method is typically much more convenient than the method described above because the analysis takes place while the system is in equilibrium. In addition, the short-time behavior of tagged particles provides an analog of the distribution of avalanches, which, unlike individual avalanches, is easily generalized to finite driving rates.

We begin by considering the long-time behavior. For the two-state models it was previously shown that the dynamics of a tagged particle suitably rescaled converges to a Brownian motion B_t, where the variance $\sigma^2\equiv(1/t)E(B_t^2)$ depends on the density and diverges as the density approaches the critical point [19]. The scaling of σ^2 for the class of two-state models with distance-dependent jump rates $c(k)\sim 1/k^{\alpha}$ can be (nonrigorously) deduced from the following calculation of the expected square jump size

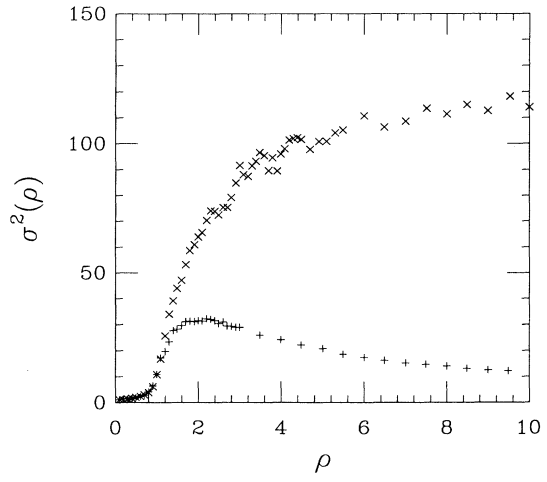

FIG. 4. Long-time behavior of tagged particles in the λ (+) and $n\lambda$ (×) models for $\lambda=128$ on the closed system. We plot the variance $\sigma^2(\rho)$ of the tagged particles as a function of ρ. Note that in each case the structure of $\sigma^2(\rho)$ mimics the behavior of the corresponding diffusion coefficient shown in Fig. 1 (a different value of λ is taken in Fig. 1). A calculation analogous to (17) for the two-state model yields a formula for the tagged particle variances for both the λ and $n\lambda$ models: $\sigma^2(\rho)=[\sum_{k=0}^{\infty}r(k)d_\rho(k)]/[\sum_{k=0}^{\infty}k\,d_\rho(k)]$, from which the respective properties can be determined analytically.

$$\sigma^2(\rho)=\sum_i k^2 c(k)\rho^{k-1}(1-\rho)\sim\frac{1}{(1-\rho)^{2-\alpha}}\ . \qquad (17)$$

The fact that the limiting distribution of the position of a tagged particle is a Brownian motion with variance σ^2 is established in Ref. [19], and is summarized in the following theorem.

Theorem. Consider any of the two-state models with jump rate $c(k)=k^{-\alpha}$, $\alpha>0$, on the integer lattice Z with initial distribution ν_ρ (product measure at density ρ) conditioned on the event that there is a particle at the origin. Denote the location of this tagged particle at time t by x_t. Then $\epsilon x_{\epsilon^{-2}t}$ converges weakly as $\epsilon\to 0$ to a Brownian motion B_t with variance σ^2 given in (17).

Remark. The order of the singularity in σ^2 is one less than that found for the corresponding diffusion coefficient $D(\rho)\sim 1/(\rho_c-\rho)^\phi$, where $\phi=3-\alpha$.

We now use tagged particles to study the λ and $n\lambda$ models introduced in Sec. II. In numerical simulations we tag a particle (or, to accelerate convergence, tag all of the particles) and accumulate data for the distribution of displacements at time $t=T$ (T large) relative to the initial position at $t=0$. Next we repeat this calculation for a variety of densities ρ. Our results for $\sigma^2(\rho)$ are plotted in Fig. 4. Comparing these results with our analytical results for the diffusion coefficient $D(\rho)$ illustrated in Fig. 1, we see that the qualitative differences between the λ and $n\lambda$ models seen first for $D(\rho)$ are preserved when we study tagged particles: at a density $\rho^*(\lambda)>\rho_c$ there is a crossover from a rapidly increasing $\sigma^2(\rho)$ to a relatively constant $\sigma^2(\rho)$ in the $n\lambda$ model and a decreasing $\sigma^2(\rho)$ in the λ model. As previously noted for the case of infinite driving rates, the singularity of $\sigma^2(\rho)$, or in this case the rate of increase in $\sigma^2(\rho)$ before the crossover at ρ^*, will

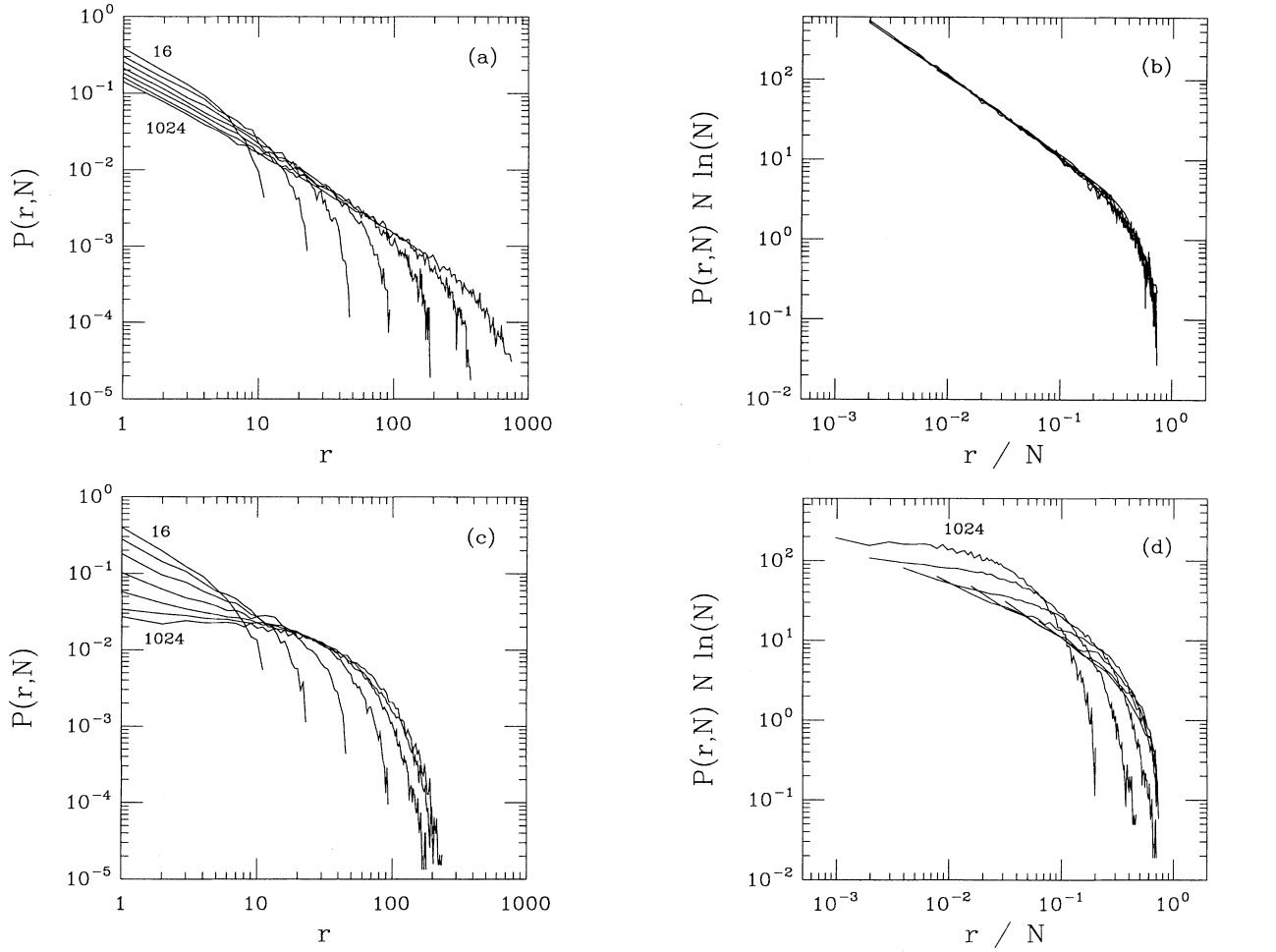

FIG. 5. Short-time displacements of tagged particles. (a) Results for the $1/k$ model for system sizes $N=16,32,64,128,256,512,1024$. We plot the probability of moving a distance r in a time $T=0.5$ (which corresponds approximately to the amount of time it takes for roughly half of the particles to attempt one event). To eliminate edge effects we consider only particles which are in the middle half of the system. We omit the probability of not moving, and normalize the remaining probabilities. (b) shows that the finite-size scaling form, which is derived analytically for the distribution of events in this model, also gives a good fit to the short-time behavior of tagged particles. (c) Short-time behavior of tagged particles in the $n\lambda$ model for $\lambda=8192$ and the same range of system sizes. For larger system sizes we begin to see the crossover to simple linear diffusion where the distribution is independent of N. (d) Finite-size scaling fit used in (b) applied to the $n\lambda$ model. Note that the smallest systems (up to about 64) collapse fairly well, but for the biggest systems the deviations become substantial.

be one order less than the corresponding divergence or increase in $D(\rho)$. Thus we are not gaining new information by this technique. Instead, the long-time behavior of tagged particles provides an alternate and more convenient method to determine the structure of the diffusion coefficient for various systems. In particular, this is the method we use in Sec. IV when we study sandpiles at finite driving rates.

The Brownian motions described above are obtained only in the limit of long times (many jumps). It is interesting to note that the short-time behavior of tagged particles looks quite different and reflects features, in particular, scaling properties, which are associated with individual avalanches. Here we consider the open system, where the density increases with system size (Fig. 3). In Ref. [8] we let $P(k,N)$ denote the probability of a jump of size k, and found that in the two-state models this distribution exhibits finite-size scaling with exponents which could be calculated exactly. In the two-state models it is reasonable to expect, and we have confirmed numerically, that the probability $P(r,N)$ that the tagged particle on a system of size N has moved distance r after some short time T has essentially the same scaling [see Figs. 5(a) and 5(b)]. For the λ and $n\lambda$ versions of the $1/k$ model, we find that as long as the density is small, $P(r,N)$ satisfies finite-size scaling with the same exponents as the $1/k$ model. This is illustrated for the $n\lambda$ model in Figs. 5(c) and 5(d). However, as in the steady-state profiles discussed in the preceding section, crossovers are observed when $N=O(\lambda^{1/2})$. For larger system sizes departures from finite-size scaling are observed, and for N sufficiently large, the $n\lambda$ model has a crossover to simple linear diffusion, where $P(r,N)$ is independent of system size N.

IV. SANDPILES AT FINITE DRIVING RATES

In this section we apply our previous techniques to a finite-driving-rate generalization of the one-dimensional limited local sandpile model introduced in Ref. [2]. This particular sandpile model has been studied in a variety of contexts because it has certain simplifying features which make it somewhat more tractable analytically and numerically [7,10,11,20]. The rules of the automaton in the limit of infinitesimal driving rates are as follows. Each site on the one-dimensional integer lattice has associated with it an integer height $h(i)$ which describes the number of grains of sand. The slope associated with each site $z(i)\equiv h(i)-h(i+1)$ is a conserved quantity on the closed system. Sand is added one grain at a time to a randomly chosen site i, so that $z(i)\rightarrow z(i)+1$ and $z(i-1)\rightarrow z(i-1)-1$. If after adding the grain the slope at site i is above a specified threshold $z(i)>z_c$, then an avalanche is triggered and m grains fall to the neighboring site $i+1$. Consequently,

$$z(i)\rightarrow z(i)-2m\ ,$$

$$z(i+1)\rightarrow z(i+1)+m\ ,$$

$$z(i-1)\rightarrow z(i-1)+m\ .$$

This relaxation mechanism is iterated: each site which is above the threshold z_c simultaneously topples. The avalanche stops when all sites are below threshold, and only then will another grain be added to the system. There are two integer parameters for the model, z_c and m (z_c is a trivial parameter in that it sets the mean slope of the system but has no effect on the distribution of events). However, as long as $m\geq 2$ it has been demonstrated that different choices of parameters lead to models which are in the same universality class [2], so from here on we will take $z_c=m=2$. The evolution of the slope configuration is well defined on a closed system (an N-site torus) for all configurations in which an avalanche does not traverse the entire system. On an open system the rules are modified at the boundaries; typically the system is closed at the left edge $i=1$, so that no sand can leave the system from that side, and open on the right edge $i=N$, where sand can flow out of the system. It is interesting to note that, in terms of *slope,* the left edge is actually the open edge since there can be no net increase or decrease in the total slope of the system unless the site $i=1$ changes height. This is clear when one notes that the average slope in the system is $\bar{z}=h(1)/N$.

Previously we showed numerically that this model is described by a singular diffusion equation analogous to Eq. (7) in which the analog of ρ is the slope density s and the order of the diffusion singularity is $\phi=4$. Subsequently this result was obtained analytically using scaling arguments and certain special features of this model [10]. In this section we examine what we believe to be the most natural generalization of the model to finite driving rates (another generalization was considered in Ref. [20]). Instead of adding grains to the system only after the avalanche is complete, we add grains at a constant rate. More precisely, at each time step all supercritical sites topple simultaneously, and to each site a grain of sand is added independently with probability $\delta>0$. In our previous notation, $\lambda=1/\delta$, so that as $\lambda\rightarrow\infty$ we retrieve the original (infinitesimal-driving-rate) sandpile model. Note that in this generalization, as well as in the original sandpile model, sites which are above threshold topple at a fixed rate regardless of how far above threshold they are, and when they topple a fixed number of grains of sand move. Thus we may expect the behavior of this system to be more analogous to the λ model than the $n\lambda$ model discussed previously.

To analyze the behavior of this model we use the long-time behavior of tagged particles. In Fig. 6 we plot $\sigma^2(s)$ as a function of the average slope s for the closed system. This is compared with the $\lambda=\infty$ result, where we observe a third-order singularity in $\sigma^2(s)$ at the critical slope $s=s_1=\frac{3}{2}$. Here we use a subscript 1, as there will be another critical value of the slope later. Notice that, like the two-state models previously discussed, the order of the singularity in σ^2 is one less than that of the diffusion coefficient. Also, note that for small values of s the behavior for finite λ mimics the singular behavior observed for $\lambda=\infty$. As in the λ model, here we observe a sharp peak in $\sigma^2(s)$ at a value $s_1^*(\lambda)>s_1$. Furthermore, we observe that $s_1^*\rightarrow s_1$ as $\lambda\rightarrow\infty$.

The most striking feature in $\sigma^2(s)$ for the finite-driving-rates sandpile model is the double-peak structure.

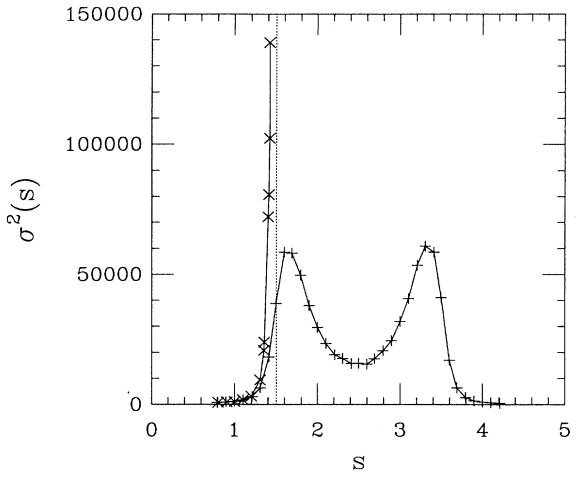

FIG. 6. Variance of tagged particles in the limited local sandpile for $\lambda=\infty$ ($\times$) and $\lambda=200$ ($+$). For $\lambda=\infty$ the variance has a cubic divergence at a critical slope $s_1=\frac{3}{2}$. For $\lambda=200$, we see the double peaks which are relics of the divergences at $\frac{3}{2}$ and $\frac{7}{2}$ discussed in the text.

This was not seen in either of our generalizations of the $1/k$ model. Here the second peak occurs at a density $s_2^*(\lambda)$, which converges to $s_2=\frac{7}{2}$ as $\lambda\to\infty$. To explain this behavior, we first recall that in the unperturbed sandpile models, *troughs* [sites with slope $z(i)\le z_c-m$] play a key role in understanding the system. It was proven [7] that troughs bound avalanches. Moreover, an avalanche has the effect of removing m units of slope from each of two sites in the interior of an interval, and depositing the slope at the two boundary troughs. On a closed system the density of troughs vanishes as the slope density increases to the critical slopes $s_1=\frac{3}{2}$. This implies that the length scale on which the slope is transported diverges as the slope increases to s_1, which explains the singularity in the diffusion coefficient. These ideas have been developed more fully in Ref. [10]. For the sandpile with finite driving rates, we begin by noting that at high slope density (that is, when most sites are toppling) the pertinent concept is one of *antitroughs.* These sites have slope $z(i)>z_c+m$, so that even after one relaxation they are still supercritical (troughs were still subcritical after one relaxation of a neighboring site).

In our finite λ extension of the sandpile model, *two adjacent supercritical sites have no net exchange of slope.* Using this convention, the model is well defined for any slope density, and configurations in which all sites have slope $z(i)>z_c$ are stable. The key observation to make is that there is a reflection symmetry about slope $\frac{5}{2}$: any configuration run through the mapping $z(i)\to 5-z(i)$, evolved according to the old rules, and reflected again, yield the same configuration as that obtained by merely evolving the configuration. The singularity which exists at $s=\frac{7}{2}$ in the limit of $\lambda\to\infty$ is an immediate consequence of this symmetry and the existence of the singularity at $\frac{3}{2}$.

The steady-state profile of the finite-driving-rates sandpile model on an open system can also exhibit the interesting structure observed in the long-time behavior of tagged particles on the closed system. In Fig. 7 we plot the time-averaged profile of the sandpile model with fixed $\lambda=200$ for varying system size. As with the two-state model and its generalizations, here we see that on the open system the average slope density increases with increasing system size (the is due to an effective forcing which scales with N rather than an increasing flux). We will refer to the left edge as open, as this is the boundary through which slope can flow (it is closed to sand), and we will refer to the right edge as closed.

For smaller systems the profile resembles the $\lambda=\infty$ case in which most of the system has a nearly constant slope s approaching s_1 with a boundary layer near $x=0$. However, as N increases the density increases, and eventually when N is of order λ we begin to explore the double peak structure of $\sigma(s)$. As illustrated in Fig. 7, for N of order λ the profile has two nearly level regions, the first near the open edge at a density near s_1 and the other near the closed edge at a density near s_2. There continues to be a boundary layer at $x=0$, and a discontinuity at $x=1$ (the point $x=1$ is anomalous and is omitted in Fig. 7). In addition, there is a sharp transition which separates the two level regions somewhere in the middle of the system. The position of this crossover depends on system size, and decreases towards $x=\frac{1}{2}$ as the system size N increases in order to accommodate the increasing slope density in the system.

This behavior can be understood by thinking about the *particle* current, which determines the toppling rate. The particle current is not constant throughout the system. Since particles are added everywhere, the particle flux through a site is proportional to its distance from the closed edge, and this implies that the toppling rates of the

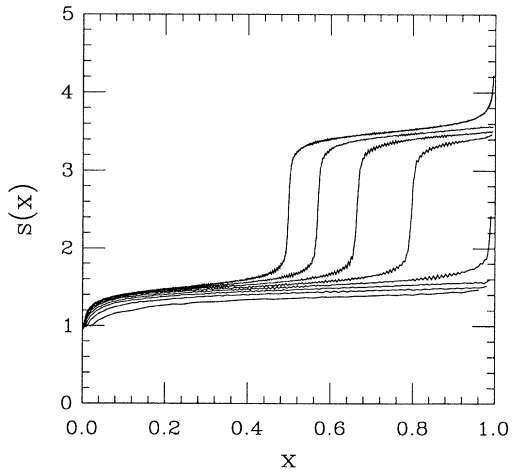

FIG. 7. Profiles of slope for the λ version of the limited local sandpile model, with $\lambda=200$ and system sizes $N=50$ (the lowest profile), 100, 150, 200, 250, 300, 350, 400, and 450 (the highest profile). For the larger values of N we see two nearly flat regions corresponding to the two peaks in the diffusion coefficient of the model. The last two profiles, as well as the profile for system size $N=800$, are seen to collapse on top of each other, except for the point at $x=1$ which is not stationary for $N>2\lambda$.

various sites are not constant. By construction, the maximum particle current off of the open edge is $m=2$, so that if the total input rate N/λ exceeds 2, any excess simply raises the total height of the sandpile. When $N=2\lambda$, the last site must always be supercritical. The site at $N/2$ where the particle current is unity must be supercritical on average half of the time. The symmetry that we have just discussed implies that at a slope of $\frac{5}{2}$ sites are supercritical on average half of the time. This means that the sites between 1 and $N/2$ will be near the lower singularity of $\frac{3}{2}$, and the sites between $N/2$ and N will be near the upper singularity of $\frac{7}{2}$ (with a boundary layer near $N/2$). For system sizes $N>2\lambda$ there is not steady-state height configuration. However, aside from $x=1$ (the open edge for sand at site N) where the slope diverges with time, the slope is well defined and has a stationary distribution which appears to be essentially the same as for the system where $N=2\lambda$.

V. CONCLUSIONS

In this paper we have introduced and studied finite-driving-rate generalizations of models which exhibit self-organized criticality in the limit of infinitesimal driving rates. In each case we have defined $\lambda=$(local transition rate)/(external driving rate). Here λ defines the separation of time scales in the models, and the original models ar retrieved in the limit $\lambda\rightarrow\infty$. For finite λ there may be flexibility in how one defines perturbations of the original model which can lead to drastically different behavior, as observed in the case of the λ and $n\lambda$ perturbations of the two-state model.

As for the self-organizing models, at finite driving rates boundary conditions play a crucial role. In the cases we have studied here, the boundary conditions lead to a monotone increase in the density with increasing system size. Consequently, for smaller systems, the steady-state profile and the scaling of the short-time, tagged particles mimic the behaviors typically found for models exhibiting self-organizing criticality. However, as system size, and therefore density, increases one observes a crossover to different behavior. Furthermore, as in the case of the sandpile model studied, this new behavior can be nontrivial. The range of system sizes for which SOC-like scaling is observed depends on λ, with a crossover occurring when there is appreciable probability that events will overlap.

In all of the cases we have studied here, we have assumed λ is fixed, and studied variations in the behavior of the system as its size N is increased. This seemed to us to be the most natural way to discuss extensions of these systems to finite driving rates. However, other scalings and the resulting limiting behaviors can also be studied. For example, Hwa and Kardar have also considered a finite-driving-rates generalization of the limited local sandpile model [20]. However, they studied the system with a fixed (small) current. In our terminology this amounts to choosing $\lambda\propto N$, while we have considered the behavior as N diverges with λ fixed. In their case the driving rate vanishes as the system size diverges. As a consequence the behavior associated with the double-peak structure we found in $\sigma(s)$ could not be discerned in their limit.

ACKNOWLEDGMENTS

The work of J.M.C. was supported by a grant from the Alfred P. Sloan Foundation and NSF Grant No. DMR-9212396. The work of E.R.G. was supported by ONR Grant No. N000014-91-J-1502. The work of G.H.S. was supported by NSA Grant No. MDA904-91-H-0018 and NSF Grant No. DMS91-03351.

APPENDIX

We begin with a discussion of the rigorous hydrodynamic limit which can be derived for the $n\lambda$ version of the $1/k$ model. Both the λ and the $n\lambda$ models are reversible with respect to one-parameter families of extremal, invariant measures indexed by the local density. First we discuss the form of the invariant measures for the general class of zero-range processes, which includes both of these systems.

Invariant measures

The state space of these models is $\{Z^+\}^Z$, so that each site on the integer lattice is either vacant or occupied by some number of particles. We will denote the configuration at time t by ζ_t. Letting $r(k)$ denote the rate at which a site with height k loses a particle in any zero-range process, in equilibrium ν_ρ the states of different sites are independent and

$$\nu_\rho\{\zeta_t(i)=k\}=\omega\frac{\beta^k}{\prod_{n=1}^k r(n)}\ , \tag{A1}$$

where ω is a normalizing constant and β is a parameter which determines the density; one must have $\beta<\liminf r(k)$[16]. A more convenient way to write ν_ρ is to let

$$\xi(k)\equiv\ln\left[\prod_{n=1}^k r(n)\right] \tag{A2}$$

and set $\alpha=\ln\beta$, so that

$$\nu_\rho\{\zeta_t(i)=k\}=\omega e^{k\alpha-\xi(k)}\ . \tag{A3}$$

The local density ρ of ν_ρ is a function of the parameter α. We will need to know $\alpha(\rho)$ in order to find $D(\rho)$. To calculate $\rho(\alpha)$, let

$$M(\alpha)=\sum_{k=0}^{\infty}e^{k\alpha-\xi(k)} \tag{A4}$$

and

$$\psi(\alpha)=\ln M(\alpha)\ ,$$

so that the density (the expected occupation number of a single site) corresponding to the invariant measure $\nu_{\rho(\alpha)}$ is given by

$$\rho(\alpha)=\psi'(\alpha)=\frac{\sum_{k=0}^{\infty}ke^{k\alpha-\phi(k)}}{\sum_{k=0}^{\infty}e^{k\alpha-\phi(k)}} . \tag{A5}$$

The function $\rho(\alpha)$ is nondecreasing. This can be seen by differentiating to obtain

$$\rho'(\alpha)=\frac{M''}{M}-\left[\frac{M'}{M}\right]^2\geq 0 , \tag{A6}$$

where the last inequality follows from Holder's inequality. When $\rho(\alpha)$ is a strictly increasing, continuous function, inverting yields

$$\alpha=(\psi')^{-1}(\rho) . \tag{A7}$$

Hydrodynamic limits

The transition mechanism is symmetric for both the λ and $n\lambda$ models, and we expect the existence of a deterministic limit under diffusion scaling for these processes. Furthermore, diffusion coefficients should converge to the singular diffusion coefficient mentioned above as we take $\lambda\rightarrow\infty$, since, at least formally, by setting $\lambda=\infty$ in both systems one recovers the two-state model with $c(k)=1/k$. This is the content of this section.

A zero-range process on the N-site torus $\mathcal{T}_N=\{1/N,\ldots,N/N\}$ has as a generator

$$L_Nf(\zeta)=\tfrac{1}{2}\sum_{i\in\mathcal{T}_N}N^2r(\zeta(i/N))[f(\eta^{i,+})-2f(\zeta)+f(\eta^{i,0})] , \tag{A8}$$

where

$$\zeta^{i,\pm}(k)=\begin{cases}\zeta(k), & k\neq i,\ i\pm1\\ \zeta(i)-1, & k=i\\ \zeta(i\pm1)+1, & k=i\pm1 .\end{cases} \tag{A9}$$

Any initial distribution of the system can be written in terms of a density f_N with respect to $\Phi_N(\zeta)\equiv\prod_{i=1}^{N}e^{-\xi(\zeta(i))}$ that is to say, initially the probability of seeing a given configuration ζ if $f_N(\zeta)\Phi_N(\zeta)$. The following conditions must hold. The first condition states that the initial distribution must converge to an initial density $\gamma(x)$ as the system size N diverges. The second condition controls the entropy of the initial distribution. If we state that each site i/N is independently occupied according to product measure at the local density $\gamma(i/N)$, where γ is a continuous function, then both conditions (i) and (ii) hold:

(i) There exists an $\gamma(x)$ so that for all $G\in C^2(\mathcal{T})$ and for any $\delta>0$,

$$\lim_{N\rightarrow\infty}P^N\left[\left|\frac{1}{N}\sum_{i=1}^{N}G\left[\frac{i}{N}\right]\zeta\left[\frac{i}{N}\right]-\int G(x)\gamma(x)dx\right|>\delta\right]=0 , \tag{A10}$$

where P^N denotes the probability measure $f_N\Phi_N$.

(ii) The following entropy bound holds for the initial distribution:

$$\int f_N\ln(f_N)\Phi_N\leq CN . \tag{A11}$$

Theorem. Consider the $n\lambda$ version of the $1/k$ model. Assume that conditions (i) and (ii) hold, and let $h(\rho)=(\psi')^{-1}(\rho)$. Let $\rho(t,x)$ be the solution of

$$\frac{\partial\rho}{\partial t}=\frac{\partial}{\partial x}\left[D(\rho)\frac{\partial\rho}{\partial x}\right] \tag{A12}$$

with

$$D(\rho)=\tfrac{1}{2}h'(\rho)e^{h(\rho)} \tag{A13}$$

with initial condition $\rho(0,x)=\gamma(x)$. Then, for any $\delta>0$,

$$\lim_{N\rightarrow\infty}\mathcal{P}^{N,f_N}\left[\left|\frac{1}{N}\sum_{i=1}^{N}G\left[\frac{i}{N}\right]\zeta_t\left[\frac{i}{N}\right]-\int G(x)\rho(t,x)\right|>\delta\right]=0 , \tag{A14}$$

where $\mathcal{P}^{N,f_N}$ denotes the measure on the path space $D([0,T],\{Z^+\}_N^{\mathcal{T}})$ with initial distribution $f_N\Phi_N$.

Remarks on Proof. With minor modifications the proof of this theorem follows that of Ref. [18], which establishes diffusion limits for systems which are essentially continuous versions of the zero-range process. The distribution of the single-site occupation number for the $n\lambda$ version has sufficiently strong exponential tails for the method to work. This is not the case for the λ model.

Calculating $D(\rho)$

This is an unpleasant task, for which there is no guarantee of getting a closed-form solution. In fact, for the $n\lambda$ model we obtain transcendental equations rather than an explicit solution.

λ model. Although the λ model was lacking exponential moments needed for the rigorous result stated above, we can still proceed to formally calculate the diffusion coefficient for this system. In this case we have $r(k)=\lambda$ for $k\geq2$ and $r(1)=1$. Therefore,

$$\xi(k)=\begin{cases}0, & k=0,1\\ (k-1)\ln(\lambda), & k\geq2\end{cases} \tag{A15}$$

so that

$$M(\alpha)=1+\frac{\lambda\beta}{\lambda-\beta} , \tag{A16}$$

where $\beta=e^{\alpha}$. With $\psi=\ln[M(\alpha)]$, we see that

$$\rho=\psi'(\alpha)=\frac{\lambda^2\beta}{(\lambda-\beta)(\lambda-\beta+\lambda\beta)} , \tag{A17}$$

from which one obtains

$$h(\rho)=[\psi']^{-1}(\rho) . \tag{A18}$$

Implicit differentiation yields

$$h'(\rho)=\frac{1}{[\psi''(\alpha(\rho))]} , \tag{A19}$$

yielding

$$D(\rho)=\tfrac{1}{2}\psi''(\alpha(\rho))]^{-1}e^{\alpha(\rho)} . \tag{A20}$$

The unpleasant result of these computations is plotted in Fig. 1.

To establish convergence to the singular diffusion for densities less than unity, expansions yield

$$\rho=\frac{\beta}{1+\beta}+O\left[\frac{1}{\lambda}\right],\quad \psi''=\frac{\beta}{(1+\beta)^2}+O\left[\frac{1}{\lambda}\right], \tag{A21}$$

from which it follows that $D_{n\lambda}(\rho)\sim\frac{1}{2}(1-\rho)^{-2}$. To confirm the high-density limit of $D_\lambda(\rho)$, observing that in the λ model $\rho\to\infty$ corresponds to $\beta\uparrow\lambda$, we have from (A17) that $\beta\sim(\lambda\rho)/(1+\rho)$. Inserting this into (A20) and expanding yields the desired result:

$$D_\lambda(\rho)\sim\frac{\lambda}{2\rho^2} . \tag{A22}$$

Additionally, the asymptotic behavior of the location of the maximum of the diffusion coefficient and the value of $D_\lambda(\rho)$ at the maximum as the driving rate λ diverges can be extracted from (A20) yielding

$$\begin{aligned}&\rho_{\max}=1+\lambda^{-1/3}+O(\lambda^{-2/3}) ,\\ &D(\rho_{\max})=\tfrac{1}{2}\lambda-\tfrac{3}{2}\lambda^{2/3}+O(\lambda^{1/3}) .\end{aligned} \tag{A23}$$

$n\lambda$ model. In this case we have $r(n)=(n-1)\lambda$ for $n\geq 2$ and $r(1)=1$. Therefore,

$$\xi(k)=\begin{cases}0, & k=0,1\\ \ln[(k-1)!\lambda^{k-1}], & k\geq 2\end{cases} \tag{A24}$$

so that

$$M(\alpha)=1+\beta e^{\beta/\lambda} , \tag{A25}$$

where again $\beta=e^{\alpha}$ and

$$\rho=\psi'(\alpha)=\frac{\beta e^{\beta/\lambda}(\beta+\lambda)}{\lambda(1+\beta e^{\beta/\lambda})} . \tag{A26}$$

The diffusion coefficient is obtained via (A20).

Convergence of $D_{n\lambda}(\rho)$ to the singular diffusion coefficient for densities less than unity follows from expansions which are the same to leading order as in the λ model in (A21), from which it follows that $D_{n\lambda}(\rho)\sim\frac{1}{2}(1-\rho)^{-2}$. To confirm the high-density limit of $D_{n\lambda}(\rho)$, observing that in the $n\lambda$ model $\rho\to\infty$ corresponds to $\beta\to\infty$, we have from (A26) that $\beta\sim\lambda\rho$, and $\psi''\sim\beta/\lambda$, from which it follows that $D_{n\lambda}(\rho)\sim\frac{1}{2}\lambda$.

[1] P. Bak, C. Tang, and K. Wiesenfeld, Phys. Rev. Lett. **59**, 381 (1987).

[2] L. Kadanoff, S. Nagle, L. Wu, and S. Zhou, Phys. Rev. A **39**, 6524 (1989).

[3] H. J. Jensen, Phys. Rev. Lett. **64**, 3103 (1990).

[4] Y. C. Zhang, Phys. Rev. Lett. **63**, 470 (1989).

[5] D. Dhar, Phys. Rev. Lett. **64**, 1613 (1990).

[6] J. M. Carlson, E. R. Grannan, G. H. Swindle, and J. Tour, Ann. Prob. (to be published).

[7] J. M. Carlson, J. T. Chayes, E. R. Grannan, and G. H. Swindle, Phys. Rev. A **42**, 2467 (1990).

[8] J. M. Carlson, J. T. Chayes, E. R. Grannan, and G. H. Swindle, Phys. Rev. Lett. **65**, 2547 (1990).

[9] J. M. Carlson, E. R. Grannan, and G. H. Swindle (unpublished).

[10] L. Kadanoff, A. Chhabra, A. Kolan, M. Feigenbaum, and I. Procaccia, Phys. Rev. A **45**, 6095 (1992).

[11] J. Krug (unpublished).

[12] H. Spohn, *Large Scale Dynamics of Interacting Particles* (Springer-Verlag, Heidelberg, 1991).

[13] If S_n denotes the location of the SRW and τ denotes the random time that it first hits either the site from which it originated or the nearest vacant site, then the optional stopping theorem (Ref. [21]) yields $ES_\tau=S_0$; this can be solved to yield the result.

[14] For the variation of the $n\lambda$ model in which the transition rate is $n\lambda$ for sites with $h(i)\geq 2$ [rather than $(n-1)\lambda$, as shown in Fig. 1] the diffusion coefficient has a peak at $\rho^*>1$, where $D\propto\lambda$ and clearly exceeds $\lambda/2$. Subsequently, D decreases to $\lambda/2$ as $\rho\to\infty$. This more novel structure arises in this case because the added transition rate for the second particle is $(2n-1)\lambda$, while after that for each additional particle the added transition rate is merely λ.

[15] The variation of the $n\lambda$ model in which the transition rate is $(n-1)\lambda+1$ for sites with $h(i)\geq 2$ has a diffusion coefficient which for large λ is essentially indistinguishable from the $D_{n\lambda}(\rho)$ shown in Fig. 1, though it is much more difficult to calculate.

[16] T. M. Liggett, Ann. Prob. **1**, 240 (1973).

[17] P. A. Ferrari, E. Presutti, and M. E. Vares, Stochastic Proc. App. **26**, 31 (1987).

[18] M. Z. Guo, G. C. Papanicolaou, and S. R. S. Varadhan, Commun. Math. Phys. **118**, 31 (1988).

[19] J. M. Carlson, E. R. Grannan, and G. H. Swindle, Stoch. Proc. Appl. (to be published).

[20] T. Hwa, Ph.D. thesis, Massachusetts Institute of Technology, 1990; T. Hwa and M. Kardar (unpublished).

[21] R. Durrett, *Probability: Theory and Examples* (Wadsworth & Brooks/Cole, Belmont, CA, 1991).